HHS Public Access

Author manuscript

Cell Microbiol. Author manuscript; available in PMC 2020 August 01.

Published in final edited form as:

Cell Microbiol. 2020 August ; 22(8): e13210. doi:10.1111/cmi.13210.

Induction of neutrophil extracellular traps (NETs) by *Campylobacter jejuni*

Sean Callahan[a], **Ryan Doster**[b], **Brittni R. Kelley**[a], **Jennifer A. Gaddy**[b], **Jeremiah G. Johnson**[a,#]

[a]Department of Microbiology, University of Tennessee, Knoxville, TN 37996, USA

[b]Division of Infectious Diseases, Department of Medicine Vanderbilt University Medical Center, Nashville, TN 37232, USA

Abstract

Campylobacter jejuni is the leading cause of bacterial-derived gastroenteritis worldwide and can lead to several post-infectious inflammatory disorders. Despite the prevalence and health impacts of the bacterium, interactions between the host innate immune system and *C. jejuni* remain poorly understood. To expand on earlier work demonstrating that neutrophils traffic to the site of infection in an animal model of campylobacteriosis, we identified significant increases in several predominantly neutrophil-derived proteins in the feces of *C. jejuni*-infected patients, including lipocalin-2, myeloperoxidase, and neutrophil elastase. In addition to demonstrating that these proteins significantly inhibited *C. jejuni* growth, we determined they are released during formation of *C. jejuni*-induced neutrophil extracellular traps (NETs). Using quantitative and qualitative methods, we found that purified human neutrophils are activated by *C. jejuni* and exhibit signatures of NET generation, including presence of protein arginine deiminase-4, histone citrullination, myeloperoxidase, neutrophil elastase release, and DNA extrusion. Production of NETs correlated with *C. jejuni* phagocytosis/endocytosis and invasion of neutrophils, suggesting that host- and bacterial-mediated activities are responsible for NET induction. Further, NET-like structures were observed within intestinal tissue of *C. jejuni* infected ferrets. Lastly, induction of NETs significantly increased human colonocyte cytotoxicity, indicating that NET formation during *C. jejuni* infection may contribute to observed tissue pathology. These findings provide further understanding of *C. jejuni*-neutrophil interactions and inflammatory responses during campylobacteriosis.

Graphical Abstract

[#]**Corresponding Author:** Jeremiah G. Johnson, MS, PhD, 516 Ken and Blaire Mossman Bldg., 1311 Cumberland Avenue, Knoxville, TN 37996, Phone: (865) 974-6229, jjohn358@utk.edu.

Author Contributions

S.C. and J.G.J. conceived and designed the experiments. S.C., R.D., and B.K. conducted the experiments. S.C. analyzed the data. S.C., R.D., and J.G.J. wrote the manuscript. All authors reviewed the manuscript.

Conflict of Interest

The authors declare no conflict of interest.

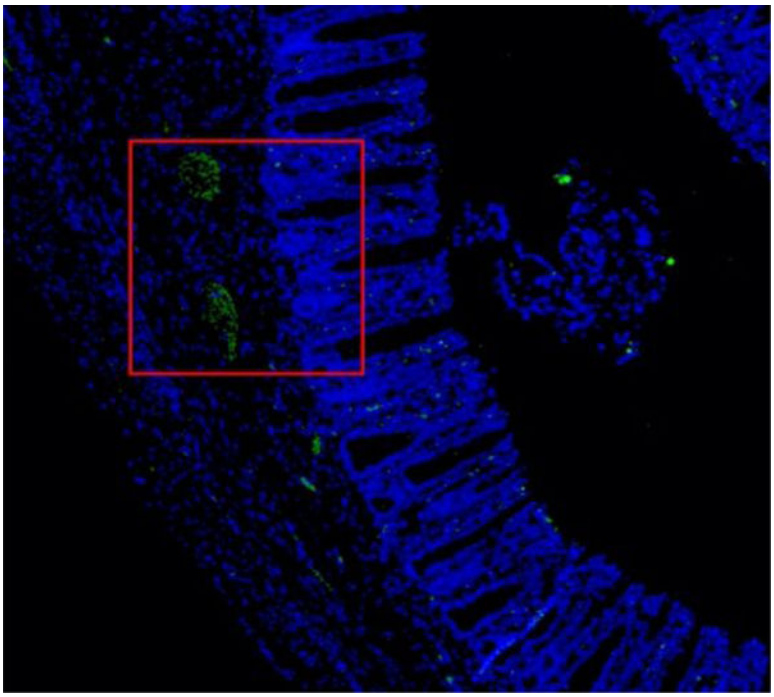

Abstract

Visualization of neutrophil extracellular traps within *Campylobacter jejuni* infected ferret tissue. These NETs are co-localized to the crypts in the intestinal tissue, providing key evidence for NET induced crypt abscess formation. Crypt abscesses have long been seen during *C. jejuni* infection, this research provides some of these answers.

Keywords

Campylobacter jejuni; neutrophils; Microbial-cell interaction; Infection; Flagella

1. Introduction

Campylobacter species are a leading cause of bacterial-derived gastroenteritis worldwide, impacting ninety-six million people annually (Man, 2011; World Health Organization, 2015). Following consumption of contaminated food or water, *Campylobacter jejuni* adheres to the intestinal mucosa, causing inflammation and tissue pathology (Backert, Boehm, Wessler, & Tegtmeyer, 2013; Stahl & Vallance, 2015). Symptoms of acute campylobacteriosis typically include inflammatory, bloody diarrhea, abdominal cramps, fever, and vomiting (Black, Levine, Clements, Hughes, & Blaser, 1988). While infection is often self-limiting and resolves after several days, numerous post-infectious disorders have been observed, including Guillan-Barré syndrome (GBS), irritable bowel disease (IBD), and reactive arthritis (ReA) (Reti, Tymensen, Davis, Amrein, & Buret, 2015). Furthermore, the rise of antibiotic resistant strains has led the Centers for Disease Control (CDC) and the World Health Organization (WHO) to classify *Campylobacter* as a serious threat to public health (Silva et al., 2011; Young, Davis, & DiRita, 2007).

Despite the global prevalence and consequences of campylobacteriosis on human health, the innate immune response to this bacterium is poorly understood when compared to other less prevalent gastrointestinal pathogens such as *Escherichia*, *Listeria, Shigella*, and *Vibrio* genera (Young et al., 2007). In both ferret and murine models of campylobacteriosis, neutrophils are recruited to infected intestinal tissue, leading to accumulation of neutrophil-derived antimicrobial proteins in the feces and tissue (Nemelka et al., 2009; Shank et al., 2018). Additionally, recruited neutrophils promote development of crypt abscesses in hyperinflammatory IL-$10^{-/-}$ mice infected with *C. jejuni* (Sun et al., 2013). Taken together, these observations suggest that neutrophils are particularly important to the development of disease and resolution of infection, but the neutrophil responses to *C. jejuni* remain uninvestigated.

Neutrophils are the most abundant leukocytes in humans and have three main antibacterial functions: (1) phagocytosis of microbes, (2) degranulation of antimicrobial proteins, and (3) extrusion of neutrophil extracellular traps (NETs) (Kolaczkowska & Kubes, 2013). After engulfment of the microbe during phagocytosis, neutrophils utilize bactericidal proteins and enzymes found within lysosomes to degrade the pathogen (Dale, Boxer, & Liles, 2008). While phagocytosis is an effective method for bacterial clearance, pathogens have developed mechanisms to invade and/or survive within neutrophils (Copenhaver et al., 2014; Fukuto & Bliska, 2014). Invasion of phagocytes by bacterial pathogens is typically induced through bacterial secretion systems. This activity has been observed for *C. jejuni* during invasion of host colonic epithelial cells where the bacterium utilizes a flagellar secretion system to invade and form *Campylobacter* containing vacuoles (CCVs) (Coburn et al., 2007; Watson & Galán, 2008). While this work has been done on epithelial cells, the ability of *C. jejuni* to invade and persist in leukocytes remain uncharacterized. During neutrophil degranulation, antimicrobial peptides are released into the external environment to limit growth and/or kill microbes localized to that region of tissue (Kolaczkowska & Kubes, 2013). Similar to degranulation, NETs are composed of extracellular DNA bound by numerous antimicrobial granule components that function to both prevent pathogen dissemination throughout the host while also restricting their growth and viability at the site of induction (V. Brinkmann, 2004; Kolaczkowska & Kubes, 2013). Bacteria have evolved strategies to specifically counteract NETs through the production of pathogen-derived DNases, which can degrade the NET and limit contact with the antimicrobial molecules present within the structure (Storisteanu et al., 2017).

While NETosis benefits the host by restricting growth and facilitating clearance of pathogenic microbes, there is increasing evidence that NET components are cytotoxic to host cells and stimulate inflammation (Saffarzadeh et al., 2012). As a result, NETs have been linked to numerous inflammatory disorders in humans, including rheumatoid arthritis (RA), irritable bowel disease (IBD), systemic lupus erythematosus (SLE), and tumor metastasis (Erpenbeck & Schön, 2017; He, Yang, & Sun, 2018; Papayannopoulos, 2018). Since several of the post-infectious disorders that occur following *Campylobacter* infection resemble these, we hypothesized that NETs are induced within the intestinal tissue during infection and may play a role in disease induction and progression.

While the neutrophil response to *C. jejuni* remains mostly uncharacterized, work has been done to understand how other immune cells recognize and respond to the pathogen. Previous work demonstrated that *C. jejuni* activates dendritic cells (DCs) through toll-like receptor 4 (TLR4), which led to B cell proliferation and antibody secretion (Kuijf et al., 2010). This finding was supported by *in vitro* experiments utilizing HEK293 TLR4 expressing reporter cells (Rathinam, Appledorn, Hoag, Amalfitano, & Mansfield, 2009). TLR4 mediates multiple activities in innate immune cells, including recognition of lipopolysaccharides (LPS) from Gram-negative bacteria. This recognition initiates a proinflammatory cascade which includes NF-κB expression and subsequent proinflammatory cytokine secretion. *C. jejuni* expresses lipooligosaccharides (LOS), which are recognized and bound by the CD14/MD2/TLR4 complex on immune cells (Kuijf et al., 2010). Interestingly, the LOS structure of *C. jejuni* is hypothesized to be a molecular mimic of human gangliosides and has been implicated in the development of GBS. To date, it is unknown whether *C. jejuni* LOS is immunogenic to neutrophils during infection. In addition to binding LPS/LOS via MD-2, TLR4 also coordinates production of immune cell endocytosis, facilitating internalization of microbes into phagocytes (Tan, Zanoni, Cullen, Goodman, & Kagan, 2015).

In this work, we expand upon earlier observations and demonstrate that neutrophil-derived proteins are readily detectable in the feces of *Campylobacter*-infected patients and that these proteins inhibit *C. jejuni* growth *in vitro*. We also found that *C. jejuni* induces NET production in primary human neutrophils and that *C. jejuni* stimulates NET production at a level similar to that of the well characterized NET inducer, *S. typhimurium*. Further, we observed that *Campylobacter* invades and/or is endocytosed by human neutrophils and that, by using non-invasive flagellar mutants or blocking TLR4-mediated endocytosis, we could successfully reduce NET induction. This indicates that host-mediated phagocytosis/endocytosis and bacterial-driven invasion may promote the release of NETs during infection. To determine whether this response occurs *in vivo*, we visualized NETs within weaning-aged ferret colon tissue during *C. jejuni* infection. Lastly, we demonstrate that NETs induced by *C. jejuni* significantly increase colonocyte cytotoxicity, indicating that the production of NETs during infection may contribute to the pathology of colon tissue.

2 Methods

2.1 Human fecal ELISA assays for neutrophil-derived proteins.

Residual human fecal samples from standard-of-care testing were obtained from the University of Nebraska Medical Center's Department of Pathology and Microbiology (approval UTK IRB-17-03795-XM). Fecal specimens were evaluated for the presence of gastrointestinal pathogens using a BioFire FilmArray Gastrointestinal Panel. Samples that did not contain detectable gastrointestinal pathogens ("uninfected") and those that tested positive for only *C. jejuni* ("infected") were used for subsequent analyses. Approximately 100 μl of liquid or 100 μg of solid feces were aliquoted into 1.5 mL microcentrifuge tubes along with 1 mL of diluent (0.1% Tween 20 solution in sterile 1X phosphate-buffered saline (PBS)). Samples were vortexed for 20 minutes then centrifuged at 12,000 rpm to isolate the supernatants (Chassaing et al., 2012). From these supernatants, 100 μl was used for

lipocalin-2 (Lcn2) (R&D Cat. DY1757–05) myeloperoxidase (MPO) (Cayman Cat. 501410), and neutrophil elastase (Ela2) (R&D Cat. DY9167–05) detection ELISAs. Absorbance values (450 nm) were determined following the manufacturer's protocol and concentrations were calculated using a standard curve of known protein concentrations. Statistical analysis was performed using a Mann-Whitney t-test with Welch's correction.

2.2 Bacterial cultures and culture conditions.

Campylobacter jejuni 81–176, enterohemorrhagic *Escherichia coli* (*EHEC*) 0157:H7, and *Salmonella typhimurium* SL1344 were stored at −80°C in MH broth supplemented with 20% glycerol. *C. jejuni* was routinely grown on Mueller-Hinton agar containing 10% sheep's blood and 10 ug/ml trimethoprim (TMP) at 37°C under microaerobic conditions (85% N2, 10% CO2, and 5% O2) for 48 hours. Where indicated, *C. jejuni* was also grown on Mueller-Hinton agar containing 10% sheep's blood, 40 μg/ml cefoperazone, 100 μg/ml cycloheximide, 10 μg/ml trimethoprim, and 100 μg/ml vancomycin (*Campylobacter*-selective). *EHEC* and *S. typhimurium* were grown on LB agar under similar microaerobic conditions for 24 hours.

2.3 *Analysis of* C. jejuni *growth in the presence of neutrophil-derived antimicrobial proteins.*

Using the neutrophil-derived antimicrobial proteins, *C. jejuni* growth was monitored when incubated with purified human Lcn2 (R&D, Cat. 1757-LC-050), MPO (R&D, Cat. 3174-MP-250), and Ela2 (Millipore, Cat. 324681–50UG). To examine for Lcn2-dependent growth inhibition, the minimum inhibitory concentration (MIC) of deferoxamine mesylate (DFOM) was first determined by adding linearly increasing concentrations from 1 μg/mL to 100 μg/mL to MH broth containing *C. jejuni* 81–176 at an optical density at 600 nm (OD600) of 0.025. Cultures were grown for 12, 24, and 48 hours under microaerobic conditions at 37°C. Next, linear concentrations of ferric enterobactin from 1 μg/mL to 10 μg/mL were added to cultures containing DFOM at the MIC until growth was fully restored for 48 hours under microaerobic conditions at 37°C. Finally, cultures containing both DFOM at the MIC and ferric enterobactin at a concentration that restored growth, were incubated with linearly increasing concentrations of Lcn2 from 1 μg/mL to 100 μg/mL added until growth decreased under microaerobic conditions at 37°C. To examine for the effects of MPO and Ela2 on *C. jejuni* growth, MH broth cultures containing *C. jejuni* 81–176 at an OD600 of 0.025 were grown in the presence of linearly increasing concentrations of these proteins from 1 μg/mL to 100 μg/mL for 12, 24, and 48 hours under microaerobic conditions at 37°C.

2.4 Isolation of primary human neutrophils.

To obtain human neutrophils, 10 mL of blood was drawn from healthy donors into heparinized Vacutainer tubes and mixed 1:1 with sterile 1X phosphate buffered saline (PBS) (approval UTK IRB-18-04604-XP) (Akhtar, Chaudhary, & He, 2010). After mixing, 10 mL of lymphocyte separation medium (Corning, Cat. 25-072-CV) was underlaid. Following centrifugation at 1400 rpm for 30 minutes, the top layers were aspirated off, leaving the red blood cell and neutrophil pellet. Pellets were resuspended in 20 mL Hanks' Balanced Salt Solution 1x (Gibco, Cat. 14025076) and 20 mL 3% dextran in 0.9% NaCl. After incubating at room temperature for 20 minutes, the upper layer was transferred to a new tube.

Following centrifugation at 400 × g for 5 minutes and aspiration of the supernatant, the pellet was washed with 20 mL ice-cold 0.2% NaCl and 20 mL ice-cold 1.6% NaCl two times. Following the final aspiration, the neutrophil pellet was resuspended in 10 mL RPMI 1640 1x (Corning, Cat. 10-040-CV). Neutrophil viability and counts were performed through Trypan blue stain (Lonza, Cat. 17–942E). Neutrophil purity was determined to be approximately 95% by flow cytometry analysis of $CD11b^{hi}$ (Biolegend, Cat. 101212) and $CD66b^{+}$ (Biolegend, Cat. 305104).

2.5 *Analysis of* C. jejuni *NET induction by flow cytometry*.

To examine for NET induction, *C. jejuni*, *EHEC*, and *S. typhimurium* were grown microaerobically at 37°C for 24 to 48 hours on MH media. Bacteria were resuspended in RPMI 1640 and incubated with neutrophils for three hours under microaerophilic conditions at an equal MOI of 50:1 (bacteria:neutrophil). Following incubation, these reactions were aliquoted into wells of a 96-well plate and centrifuged at 400 × g. Pelleted cells were washed three times with sterile 1x PBS cells before incubation with Live/Dead NIR stain (Thermo, Cat. L10119) for 25 minutes at room temperature. After incubation, cells were blocked with 1% goat serum for 10 minutes, then incubated with CD11b (Biolegend, Cat. 101212) myeloperoxidase (Biolegend, Cat. 347201), CD63 (Biolegend, Cat. 353007), and Cit-H3 (Novus, Cat. NB100–57135SS and Biolegend, Cat. 406403) antibodies for 30 minutes (Zharkova et al., 2019). Cells were subsequently fixed in fixation buffer (Biolegend, Cat. 420801) for 10 minutes at room temperature and stored at 4°C until flow cytometry analysis. TLR4 was blocked with 50 μl of TLR4 neutralizing antibody (InvivoGen, Cat. pab-hstlr4) and incubated for one hour. Flow cytometry preparation was performed as stated above. Samples were analyzed using an LSR II flow cytometer and data was processed using FlowJo software. Statistical analysis was performed using unpaired t tests and significance inferred at $p < 0.05$.

2.6 Western blot analysis of NET products.

After the NET induction protocol described above, cells from three healthy volunteers were lysed with Laemmli buffer with beta-mercaptoethanol and boiled for 10 minutes. 10 μl whole cell lysate samples were loaded onto a 12.5% SDS-PAGE gel and run for 1.25 hours at 140V at room temperature. Separated proteins were transferred to nitrocellulose membranes (GE Healthcare, Cat. 10600011) for 1.5 hours at 0.25A using a semi-dry transfer apparatus. Membranes were blocked in 5% milk in TBS-T for 60 minutes shaking. To probe for proteins of interest, 1:5000 dilution rabbit anti-human Lcn2 (Invitrogen, Cat. 702248), 1:5000 dilution mouse anti-human Ela2 (R&D, Cat. MAB91671), 1:5000 dilution goat anti-human MPO (R&D, Cat. AF3174), 1:1000 dilution rabbit anti-human PAD4 (Thermo, Cat. PA5–12236), 1:5000 dilution rabbit anti-human Cit-H3 (Novus, Cat. NB100–57135SS) and 1:500 dilution mouse anti-human β-actin (Biolegend, Cat. 643801) were incubated on individual membranes for 1 hour at room temperature with shaking. Membranes were subsequently washed three times with filtered TBS-T for 5 minutes each. Proteins of interest were detected using a 1:2000 dilution of appropriate horseradish peroxidase conjugated secondary antibodies in 15 mL 5% milk in TBS-T and incubated for 45 minutes at room temperature with shaking. Membranes were then washed three times with filtered TBS-T, shaking for 5 minutes each. After the final wash, membranes were developed with a solution

containing 5 mL peroxide and 5 mL luminol/enhancer solution (Thermo, Cat. 34580) and incubated for 5 minutes at room temperature with shaking. A *C. jejuni* negative control was also performed to ensure there was no cross-reactivity and no detection of proteins was noted. Chemiluminescent bands were imaged using the ChemiDoc-It Imager and densitometry measurements were made using ImageJ software. Statistical analysis was performed using unpaired t tests and significance inferred at $p < 0.05$.

2.7 *Analysis of* C. jejuni *NET induction by SYTOX assay*.

Following the *C. jejuni* NET induction described above, cells were added to wells of black 96-well plates (Invitrogen, Cat. 655077–25) and centrifuged at 400 × g. Supernatants were discarded and 1.0 μM SYTOX Green (Invitrogen, Cat. S7020) was added to each sample and incubated under microaerobic conditions at 37°C for one hour (Volker Brinkmann, Laube, Abu Abed, Goosmann, & Zychlinsky, 2010). After incubation, cells were centrifuged at 400 × g and the supernatant was discarded. The cells were washed once with 1x PBS and then resuspended in 100 μl 1x PBS. SYTOX fluorescence was measured at 504/523 nm using a BioTek plate reader. Statistical analysis was performed using unpaired t tests and significance inferred at $p < 0.05$.

2.8 Visualization of C. jejuni NET induction by fluorescence microscopy.

C. jejuni NET induction described above occurred on poly-l-lysine coated glass coverslips (Corning, Cat. 354085) for three hours at 37°C under microaerobic conditions (Volker Brinkmann et al., 2010). Following three 1x PBS washes, coverslips were incubated with a goat anti-myeloperoxidase (R&D, Cat. AF3174) and donkey anti-goat Alexa Fluor 405 (AbCam, Cat. Ab175664). Coverslips were also incubated with a mouse anti-neutrophil elastase (R&D, Cat. MAB91671) and goat anti-mouse Alexa Fluor 594 (Biolegend, Cat. 405326). After three 1x PBS washes, coverslips were incubated with 1.0 μM SYTOX Green (Invitrogen, Cat. S7020). Finally, after three 1x PBS washes, coverslips were placed on glass slides with a drop of Mowiol mounting medium (Sigma, Cat. 81381–50G) and kept in the dark at 4 °C until fluorescent microscopy was performed. Ten fields of each sample condition were visualized using a Nikon E600 Eclipse at the Advanced Microscopy and Imaging Center at the University of Tennessee. For statistical analysis, three individual neutrophil isolations were performed and stained as described above. Of those, 100 fields were observed for the presence of fluorescent NETs. Statistical analysis was performed using unpaired t tests and significance inferred at $p < 0.05$.

2.9 *Analysis of* C. jejuni *internalization by neutrophils*.

C. jejuni and neutrophils were incubated at an MOI of 10:1 for 1, 2, and 3 hours at 37°C under microaerobic conditions. Additionally, neutrophils where indicated were incubated with 2μM cytochalasin-D (CD) (Sigma, Cat. C8273–1MG) or 50 μl of TLR4 neutralizing antibody (Invivogen, Cat. pab-hstlr4). Following incubation, cells were incubated in 100 μl RPMI 1640 containing 10% FBS and 100 μg/mL gentamicin sulfate (Negretti & Konkel, 2017). This concentration of gentamicin was determined as the highest concentration that killed extracellular bacteria but did not kill internal bacteria or negatively impact neutrophil viability. After treatment, neutrophils were washed three times with 1x PBS to remove remaining antibiotic and neutrophils were lysed with 0.1% Triton X-100 for 5 minutes to

release intracellular bacteria. Three 1x PBS washes were then performed to remove excess Triton X-100. Cell pellets were resuspended in MH broth and serial dilutions were plated on *Campylobacter*-selective media. Cultures were grown for two days at 37°C under microaerobic conditions and CFUs were counted. Statistical analysis was performed using unpaired t tests and significance inferred at $p < 0.05$.

2.10 *Infection of ferrets with* C. jejuni.

As previously described, *C. jejuni* 81–176 was grown on MH + TMP and Gram strained to ensure culture purity prior to inoculation (Shank et al., 2018). This culture was streaked on *Campylobacter*-selective media and incubated at 37°C under microaerophilic conditions for 48 hours. Suspensions of *C. jejuni* 81–176 were made in sterile PBS and diluted to an OD600 of 2.0. Three male ferrets were anesthetized with isoflurane and inoculated via orogastric tube with 5 mL of *C. jejuni* 81–176 inoculum - an infectious dose of 1.5×10^9 CFU - which was combined with 5 mL of 5% sodium bicarbonate buffer prior to administration (UTK IACUC protocol #2519). Additionally, three male ferrets were mock infected with 5 mL of sterile 1X PBS which was combined with 5 mL of 5% sodium bicarbonate buffer prior to inoculation. Morphine was administered intraperitoneally to each ferret one-hour following inoculation and ferret blood was collected from the vena cava into EDTA-treated vacutainers at three days post infection. Neutrophils were isolated by density gradient centrifugation and ACK osmotic red blood cell lysis (Akhtar et al., 2010). Ferrets were subsequently sacrificed by cardiac puncture of barbiturate.

2.11 *Histologic analysis of ferret intestinal tissue during* C. jejuni *infection.*

The terminal 1 cm of the ferret colon was removed following sacrifice, and the lumen was washed five times with 1 mL of sterile, cold 1X PBS. Tissue was placed in 10% buffered formalin and fixed for 4 hours at room temperature. Fixed tissue was embedded in formalin, and 4 μm sections were stained with hematoxylin and eosin (H&E). Stained slides were visualized through bright-field microscopy, and representative images are presented. Inflammation scoring was performed as described in a blind manner, noting edema, presence of blood, hyperplasia, loss of goblet cells, epithelia raggedness, and neutrophil infiltration (Lebeis, Powell, Merlin, Sherman, & Kalman, 2009). Statistical analysis was performed using unpaired t tests and significance inferred at $p < 0.05$.

2.12 Immunofluorescence staining of ferret colonic tissue for NETs.

Ferret colon tissues were stained for the presence of NETs as previously described (Brinkmann et al., 2016; Doster et al., 2018). Tissues were deparaffinized and incubated in R universal Epitope Recovery Buffer (Electron Microscopy Sciences) at 50°C for 90 minutes. Samples were then rinsed in deionized water three times followed by washing with TRIS-buffered saline (TBS, pH 7.4). Samples were permeabilized for 5 minutes with 0.5% Triton X100 in TBS at room temperature followed by 3 washes with TBS. Samples were then blocked with TBS with 10% BSA for 30 minutes prior to incubation with 1:50 dilutions of rabbit poly-clonal anti-neutrophil elastase antibodies (MilliporeSigma, Cat. 481001). The following day, samples were washed in TBS followed by repeat blocking with blocking buffer for 30 minutes at room temperature before incubation with 1/00 dilution of Alexa Fluor® 488 conjugated donkey anti-rabbit IgG (Invitrogen) for 4 hours at room temperature.

Samples were then washed and incubated with 5 μM Hoechst 33342 for 30 minutes to stain DNA/nuclei. After final washes, slides were dried and cover slipped. Tissues were visualized with a Zeiss LSM 710 META Inverted Laser Scanning Confocal Microscope. Images presented are composites of z-stacked images.

2.13 HCT116 Cytotoxicity in response to C. jejuni induced NETs

HCT116 cells were routinely cultured in 75 cm^2 flasks in 10 mL of DMEM supplemented with 10% FBS, 100 U/mL Pen-Strep antibiotics, and 2 mM L-glutamate at 37°C and 5% CO_2. 6×10^4 cells were then seeded in 96 well plates to adhere overnight. After neutrophils were incubated with *C. jejuni* to allow NETosis as previously described, *C. jejuni*-neutrophil pellets were incubated with HCT116 cells for 24 hours at 37°C and 5% CO_2. Following incubation, the plate was centrifuged at 250 × g for three minutes. 50 μL of culture supernatant was then plated on another 96 well plate and an LDH assay was performed as described by the Pierce™ LDH Cytotoxicity Assay Kit protocol (Thermo, Cat. 88954). In brief, supernatant of the cell incubation was taken off and added to a new well. To the well, reaction mixture was added and incubated at room temperature for thirty minutes. Following incubation, stop solution was added to the well to stop the reaction from proceeding. The 96 well plate was read at the absorbances 490 nm and 680 nm. Percent cytotoxicity was calculated through the equation: [(Experimental value – Effector Cells Spontaneous Control – Target Cells Spontaneous Control) / (Target Cell Maximum Control – Target Cells Spontaneous Control)] * 100. Statistical analysis was performed using unpaired t tests and significance inferred at $p < 0.05$.

3 Results

3.1 *Neutrophil-derived proteins accumulate in feces of* C. jejuni-*infected individuals and negatively impact* C. jejuni *growth* in vitro.

Using fecal samples from *C. jejuni*-infected individuals, concentrations of lipocalin-2 (Lcn2) (Fig. 1A), myeloperoxidase (MPO) (Fig. 1B), and neutrophil elastase (Ela2) (Fig. 1C) were measured using protein-specific ELISAs. In uninfected individuals, the mean Lcn2 concentration was determined to be $3.82\times10^5 \pm 3.63\times10^5$ pg/mL, while infected individuals exhibited a significant increase with a mean concentration of $1.51\times10^6 \pm 3.15\times10^5$ pg/mL. MPO concentration of uninfected individuals was observed at a mean concentration of $1.29\times10^3 \pm 1.30\times10^3$ pg/mL and infected individuals exhibited a significant increase with a mean concentration of $3.94\times10^4 \pm 2.86\times10^3$ pg/mL. Lastly, Ela2 in uninfected fecal samples was detected at a mean concentration of $5.88\times10^2 \pm 8.61\times10^1$ pg/mL while infected samples demonstrated significant increases with a mean concentration of $1.67\times10^3 \pm 6.93\times10^2$ pg/mL. These represent approximate fold increases of 3.97, 30.47, and 2.85 for Lcn2, MPO, and Ela2, respectively. Increases in these proteins led us to hypothesize that neutrophil degranulation and/or NET production are occurring at the host-pathogen interface during human infection. In summary, we have shown that *C. jejuni* infected individuals' stool samples contain higher levels of proteins Lcn2, MPO, and Ela2.

Since Lcn2, MPO, and Ela2 were elevated in infected stool samples, we examined whether these proteins could inhibit *C. jejuni* growth *in vitro.* When purified components (Lcn2,

MPO, and Ela2) were incubated with *C. jejuni*, bacterial growth was significantly reduced, especially during the exponential phase. When cultures were grown in iron-restricted media supplemented with 3.125 mM ferric-enterobactin and 42.375 μg/mL Lcn2, mean *C. jejuni* growth (OD_{600}) significantly decreased from 0.13 ± 0.014 to 0.068 ± 0.018, 0.183 ± 0.008 to 0.096 ± 0.015, and 0.26 ± 0.01 to 0.14 ± 0.04 at 12, 24, and 48 hours when compared to iron-restricted cultures containing ferric-enterobactin (Fig. 1D). When incubated in the presence of MPO at a concentration of 73 μg/mL, *C. jejuni* growth (OD_{600}) significantly decreased from 0.11 ± 0.01 to 0.094 ± 0.011, 0.21 ± 0.008 to 0.13 ± 0.008, and 0.35 ± 0.03 to 0.19 ± 0.003 at 12, 24, and 48 hours, respectively (Fig. 1E). Finally, when incubated with Ela2 at a concentration of 25 μg/mL, the *C. jejuni* mean growth (OD_{600}) significantly decreased from 0.17 ± 0.026 to 0.086 ± 0.0015, 0.29 ± 0.018 to 0.11 ± 0.0006, and 0.34 ± 0.026 to 0.12 ± 0.007 at 12, 24, and 48 hours respectively (Fig. 1F). These represent approximately 2–3 fold reductions in growth at each time point tested for all antimicrobial proteins. Finally, these granule proteins work in concert to synergistically decrease *C. jejuni* growth (Fig. 1G). Consequently, we hypothesize that the increase of these antimicrobial proteins during human infection may aid in *C. jejuni* clearance by inhibiting *C. jejuni* growth at or within the gastrointestinal tissue.

3.2 *Purified human neutrophils interacting with* C. jejuni *exhibit markers of activation and NET formation.*

To understand neutrophil responses to *C. jejuni*, flow cytometry was utilized to determine neutrophil activation and response. When neutrophils were incubated with varying multiplicities of infection (MOIs) of *C. jejuni*, neutrophil activation and response was determined to be population density dependent. The highest activated population ($SSC^{high}CD11b^{+}MPO^{+}$) was observed at an MOI of 1:50 (neutrophil:*C. jejuni*) with a mean MFI of $1.76\times10^{5} \pm 2.74\times10^{3}$ using the flow cytometry analysis described below (Fig. 2A). Further, when this MOI was incubated with neutrophils for varying amounts of time, the highest activated population was observed at three hours using the same flow cytometry analysis with a mean MFI of $3.21\times10^{4} \pm 2.97\times10^{2}$ (Fig. 2B). These results indicate that neutrophils are activated in response to *C. jejuni* in a dose and time dependent manner.

To assess the cellular response of activated human neutrophils to *C. jejuni*, flow cytometry was similarly performed on purified human neutrophils that were incubated with *C. jejuni* and analyzed using SSC^{high}, CD11b, MPO, CD63, and citrullinated histone 3 (Cit-H3) as markers of NET formation. After incubation with *C. jejuni*, there was a significant increase in the population of mean fluorescence intensity (MFI) of $CD11b^{+}$ neutrophils from uninfected human neutrophils ($6.06\times10^{3} \pm 2.78\times10^{2}$) to infected human neutrophils ($1.21\times10^{4} \pm 3.06\times10^{2}$) (Fig. 2C). There was a subpopulation of $CD11b^{+}$ neutrophils that also stained as MPO^{+} in the absence of permeabilization and this population significantly increased when neutrophils were uninfected ($2.73\times10^{2} \pm 11.55$) and then infected with *C. jejuni* ($3.96\times10^{2} \pm 1.53$) (Fig. 2D). Additionally, there was a significant increase in $CD63^{+}$ neutrophils ($1.38\times10^{4} \pm 3.6\times10^{3}$) when infected with *C. jejuni* ($5.92\times10^{4} \pm 3.41\times10^{3}$) (Fig. 2E). Similarly, neutrophils exposed to *C. jejuni* were more frequently Cit-H3 ($2.22\times10^{3} \pm 43.7$) positive when compared to uninfected neutrophils ($5.88\times10^{2} \pm 99.0$) (Fig. 3F). These data suggest that upon activation, neutrophils were increasingly decorated with extracellular

MPO, CD63, and Cit-H3. When subpopulations of $CD11b^{+}MPO^{+}$ and $CD63^{+}Cit\text{-}H3^{+}$ cells were analyzed using LIVE/DEAD™ Fixable Near-IR (NIR) stain, cells in these populations were found to be more frequently positive, indicating that neutrophils stimulated by *C. jejuni* undergo 'suicidal' NETosis.

3.3 C. jejuni-*stimulated human neutrophils exhibit increases in several established NET components*.

To further determine whether neutrophils form extracellular traps in response to *C. jejuni*, NET components were quantitatively analyzed by western blot. Neutrophils isolated from three healthy volunteers were infected with wild-type *C. jejuni* and whole cell lysates were examined for the presence of lipocalin-2 (Lcn2), myeloperoxidase (MPO), neutrophil elastase (Ela2), peptidylarginine deiminases 4 (PAD4), and citrullinated histone 3 (Cit-H3) (Fig. 3A). Using β-actin abundance as an internal control, mean relative abundances for each protein in unstimulated neutrophils were determined by densitometry: Lcn2 (0.23 ± 0.23), MPO (0.29 ± 0.23), Ela2 (0.61 ± 0.29), PAD4 (0.016 ± 0.007), and Cit-H3 (0.071 ± 0.048). Using PMA stimulated neutrophils as a positive control for NET production, mean relative protein levels were: Lcn2 (1.41 ± 0.43), MPO (1.53 ± 0.21), Ela2 (2.51 ± 0.29), PAD4 (0.043 ± 0.006), and Cit-H3 (0.88 ± 0.32). These represent significant increases in all proteins examined with the exception of PAD4. *C. jejuni*-stimulated neutrophils exhibited increased mean relative protein levels of Lcn2 (1.11 ± 0.34), MPO (1.37 ± 0.22), Ela2 (2.55 ± 0.75), PAD4 (0.86 ± 0.16), and Cit-H3 (0.72 ± 0.35) (Fig. 3B). These abundances represent significant increases when compared to unstimulated neutrophils, with most increases between 4.1 to 4.8 fold and an increase of 10.1 fold for PAD4 expression. These increases were similar for PMA-induced neutrophils, except for PAD4 abundance. Finally, to quantify extracellular DNA extruded during *C. jejuni*-induced NETosis, a SYTOX Green assay was performed to quantify extracellular DNA and dead cells. When incubated with *C. jejuni*, a significant increase in extracellular DNA was observed as the mean relative fluorescence units (RFUs) for unstimulated neutrophils (7.43 ± 4.32) increased to 61.57 ± 9.07 when stimulated with *C. jejuni*. The amount of extruded DNA in response to *C. jejuni* stimulation was not significantly different when compared to PMA-induced neutrophils (71.14 ± 13.28) (Fig. 3C). As an additional control, we confirmed that *C. jejuni* lysates did not cross-react with any of the above antibodies (Lcn2, MPO, Ela2, PAD4, and Cit-H3) nor did it exhibit significant fluorescence when stained with SYTOX (data not shown). Therefore, these indicate that human neutrophils exhibit numerous markers of NETosis following interaction with *C. jejuni*.

3.4 C. jejuni-*stimulated human neutrophils exhibit morphological changes consistent with NET formation*.

To further confirm that NET production occurs during the neutrophil response to *C. jejuni*, immunofluorescence microscopy was performed using antibodies directed against human NET components as well as SYTOX Green to stain extruded DNA. Following examination of 100 fields, unstimulated neutrophils were found to possess intact, multi-lobed nuclei, punctate MPO staining (presumed MPO contained within granules), and low levels of Ela2 that were contained within the neutrophil border. After stimulating with *C. jejuni*, a proportion of neutrophils exhibited fewer compact nuclei with some extruding extracellular

DNA that co-localized with MPO and Ela2 (Fig. 4A). Using this morphology to designate a NETosing cell, examination of 100 fields indicated that approximately 17% of neutrophils formed NET structures at 3h post challenge (Fig. 4B). This result supported our flow cytometry-based analysis above, causing us to conclude that human neutrophils produce NETs in response to *C. jejuni* and that they contain antimicrobial proteins that can inhibit *C. jejuni* growth.

3.5 C. jejuni *induces NETs at levels higher than* E. coli O157:H7, *but comparable to* S. typhimurium.

To compare the *C. jejuni*-induced NET response to other gastrointestinal pathogens, NET induction was quantitatively compared between *E. coli* O157:H7, *S. typhimurium* SL1344, and *C. jejuni* 81–176 at the same MOI of 1:50 (neutrophil:*C. jejuni*) for three hours. *E. coli* O157:H7 has been found to not induce NETs while *S. typhimurium* has been shown to be a potent NET inducer (Brinkmann et al, 2004). Using flow cytometry and SYTOX assays described above, we confirmed previous results and found that *E. coli* O157:H7 incubation with purified human neutrophils resulted in only slight increases in the $CD11b^{+}MPO^{+}$ neutrophil population MFI ($1.17\times10^{4} \pm 2.08\times10^{3}$) while *S. typhimurium* SL1344 induced significant increases in the $CD11b^{+}MPO^{+}$ neutrophil population MFI ($1.67\times10^{4} \pm 3.05\times10^{3}$). Similarly, incubation with *C. jejuni* increased the $CD11b^{+}MPO^{+}$ neutrophil population MFI to one comparable to what was observed for *S. typhimurium* (Fig. 5A) ($2.13\times10^{4} \pm 3.21\times10^{3}$). These results were further supported by assaying DNA extrusion using SYTOX Green with mean RFUs of: *E. coli* O157:H7 (7 ± 1), *S. typhimurium* SL1344 (18.33 ± 1.15), and *C. jejuni* 81–176 (23.33 ± 3.22) (Fig. 5B). These results support our conclusions that *C. jejuni* induces NETs and that the magnitude of induction is at least comparable to *S. typhimurium* if not higher.

3.6 C. jejuni *is internalized by human neutrophils.*

One notable difference between *E. coli* O157:H7 and *S. typhimurium* is that *E. coli* O157:H7 is largely regarded as non-invasive while *S. typhimurium* is understood to be a highly invasive pathogen. To assess whether *C. jejuni* can be efficiently internalized into human neutrophils, and whether this may be a mechanism for NET induction, we leveraged gentamicin protection assays. In a control experiment, human neutrophils were incubated with *C. jejuni* at an MOI of 1:10 (neutrophils:*C. jejuni*), a concentration shown to not induce NET formation (Fig. 2A), for varying time points. *C. jejuni* was efficiently internalized into neutrophils within one hour with a mean CFU/mL of $6.67\times10^{6} \pm 5.77\times10^{5}$, representing an approximately 4-$\log_{10}$ increase when compared to the zero-hour time point (Fig. 6A). Similar results have been observed in other studies using human-derived epithelial cell lines (Neal-McKinney & Konkel, 2012). Interestingly, once internalized, the number of viable *C. jejuni* cells remains constant with $5.33\times10^{6} \pm 5.77\times10^{5}$ CFU/mL at three hours of infection, suggesting that *C. jejuni* can counteract the bactericidal effects of the neutrophil phagosome (Fig. 6A). Lastly, to determine whether neutrophil internalization was dependent on actin polymerization, we incubated human neutrophils with the actin polymerization inhibitor, cytochalasin-D. The incorporation of this inhibitor significantly reduced the number of internalized bacteria from $6.67\times10^{6} \pm 5.77\times10^{5}$ to $9.33\times10^{3} \pm 1.53\times10^{3}$ CFU/mL at hour one (Fig. 6B).

Since actin polymerization-dependent internalization may be mediated by the host cell through phagocytosis/endocytosis or the bacterium through invasion, we examined the effects of each on *C. jejuni* numbers within neutrophils. Previous work demonstrated that endocytosis of bacteria by neutrophils is dependent on interaction with TLR4 (Prokhorenko, Zubova, Kabanov, Voloshina, & Grachev, 2012). Using a commercially available TLR4-blocking antibody, internalized wild-type *C. jejuni* CFUs/mL significantly decreased from $1.12\times10^7 \pm 3.52\times10^6$ to $1.63\times10^5 \pm 2.08\times10^4$, indicating that host-directed endocytosis may contribute to bacterial entry (Fig. 6B). In addition, we incubated human neutrophils with the invasion-deficient *C. jejuni* Δ*flgE* mutant, finding that mean viable CFUs/mL significantly decreased to $2.57\times10^5 \pm 2.52\times10^4$ (Fig. 6B). As a result of these data, we concluded that *C. jejuni* internalization by human neutrophils is both dependent on TLR4-mediated phagocytosis/endocytosis and flagella-mediated bacterial invasion.

To determine whether internalization is responsible for NET induction, we used the combination of reagents above to examine whether production of NETs was negatively impacted. Using DNA extrusion as an output of NETosis, TLR4 blocking significantly decreased from 10 ± 2.08 to 2.11 ± 2.79 RFUs, representing an approximately 5-fold decrease in extracellular DNA. Further, when neutrophils were incubated with *C. jejuni* Δ*flgE*, DNA extrusion significantly decreased to 1.39 ± 0.92 RFUs (Fig. 6C). This data suggests that inhibiting TLR4-mediated endocytosis or flagella-directed *C. jejuni* invasion may reduce NET production during *C. jejuni* infection.

3.7 C. jejuni-*infected ferrets exhibit several markers of intestinal inflammation, including the accumulation of neutrophils undergoing NETosis.*

In previous work, we demonstrated that granulocytes (presumed neutrophils) and monocytes (presumed macrophages) accumulate in *C. jejuni*-infected ferret colons (Shank et al., 2018). Neutrophils from uninfected ferrets were incubated with C. jejuni, similar to above. There was a significant increase in the population of $CD11b^+$ neutrophils ($3.16\times10^4 \pm 8.86\times10^2$) when compared to those incubated with *C. jejuni* ($9.69\times10^4 \pm 1.36\times10^4$) (Fig. 7A). Further, $CD11b^+$ neutrophils stained as MPO^+ in the absence of permeabilization significantly increased from $2.43\times10^2 \pm 1.22\times10^2$ for uninfected neutrophils to $8.06\times10^2 \pm 18.5$ for infected ferret neutrophils (Fig. 7B). This demonstrated that ferret neutrophils become similarly activated in response to *C. jejuni* when compared to human neutrophils. As a result, ferrets were infected with 1.5×10^9 CFU orally and sacrificed at day three post infection, the day at which our previous studies indicated peak infection and inflammation. Infected ferrets exhibited mean *C. jejuni* loads of $1.26\times10^5 \pm 2.17\times10^4$ CFU/g of feces, while mock-infected ferrets did not yield detectable colonies (limit-of-detection: 2,000 CFU/g) (Fig. 7C). To expand upon those findings, we evaluated H&E stained colonic tissue from these animals for signs of inflammation, including edema, presence of blood, hyperplasia, loss of goblet cells, epithelia raggedness, and neutrophil infiltration (Fig. 7D). Using double blind inflammation scoring, all categories were increased in infected ferret colons when compared to the mock-infected controls (Supplemental Information). Based on these observations, increases in neutrophil abundance correlated with increased inflammation and histopathology.

Since H&E staining is unable to detect *in vivo* NETs, we sought to determine if NETs released by neutrophils in response to *C. jejuni* infection could be visualized *in vivo*. We interrogated ferret colon tissues with immunofluorescence staining for Ela2 and DNA. At low power, collections of Ela2 staining were seen just below the crypts in the colonic mucosa of infected animals. Higher magnification imaging of these collections demonstrated elongated structures with co-localized staining for both Ela2 and DNA, suggesting these structures are NETs, potentially within a crypt abscess (Fig. 7E, orange box). This was in contrast to Ela2 positive cells seen within the villi in infected tissues and throughout uninfected tissues that had well-defined nuclei and punctate Ela2 staining (Fig.7E, green boxes).

3.8 C. jejuni -*neutrophil interaction causes apoptosis of colonocytes*.

One common histologic characteristic of *C. jejuni*-infected individuals is disruption of the intestinal epithelial barrier, including the neutrophil-dependent formation of intestinal crypt abscesses (Sun et al., 2013). To determine whether *C. jejuni*-induced NETs may be responsible for epithelial barrier disruption and crypt abscess formation, we sought to quantify the cytotoxic potential of these NETs on human colonocytes. Using an LDH assay, *C. jejuni* was incubated with neutrophils to induce NET formation prior to the products being incubated for 24h with human colonocytes (HCT116). When compared to *C. jejuni*-only (0.08 ± 0.79%) or neutrophil-only controls (0.1% ± 0.09%), there was a significant increase in mean LDH release from the human colonocytes (7.64% ± 2.21%) (Fig. 7F). This release of LDH was determined to be from HCT116 cells, as a neutrophil only control resulted in minimal LDH release. Therefore, the production of NETs in response to *C. jejuni* infection may lead to colonocyte cytotoxicity and contribute to the tissue damage observed in *C. jejuni*-infected patients.

4 Discussion

Campylobacter jejuni has been recognized as the most common cause of bacterial-mediated diarrheal disease in the world (Man, 2011). Following ingestion of contaminated food or water, it is suspected that the bacterium adheres to the intestinal epithelium at the mucosal surface to induce a mild to severe inflammatory response. Surprisingly, compared to less prevalent gastrointestinal pathogens, the inflammatory process during campylobacteriosis is not well understood. Using the ferret model of campylobacteriosis, our group recently demonstrated that innate immune cells are recruited to intestinal tissue during infection and that a single neutrophil-derived protein (S100A12) could be detected in ferret feces (Shank et al., 2018). Since these results indicate that neutrophils may be important during acute disease, we sought to further characterize the response of neutrophils during *C. jejuni* infection using both *ex vivo* and *in vivo* models.

We initially observed increases in multiple, predominantly neutrophil-derived antimicrobial proteins (Lcn2, MPO, and Ela2) in the feces of infected patients (Kolaczkowska & Kubes, 2013). While many of these proteins are not exclusive to neutrophils, the repeated abundance of these proteins - in addition to our earlier results with S100A12 - supports the conclusion that neutrophils are present at relatively high abundance at the host-pathogen

interface (Shank et al., 2018). Some variability was noted among infected patient samples, which may have arisen due differences in time from when symptoms initiated to when samples were collected. Of the proteins assayed, Lcn2 has been shown to bind ferric-enterobactin and may serve to restrict iron acquisition by the bacterium (Bachman, Miller, & Weiser, 2009). Recent data from a *C. jejuni* human feeding study indicated that several iron acquisition systems are upregulated during infection, suggesting that iron may be limited within infected intestines (Crofts et al., 2018). Whether iron restriction is mediated solely through Lcn2 remains to be investigated. MPO is antimicrobial as it produces compounds, including hypochlorous acid, which are highly toxic to bacteria, virus-infected cells, and fungi (Klebanoff, 2005). Ela2 is a serine protease that can directly kill bacteria, generate antimicrobial peptides, and inactivate virulence factors (Weinrauch, Drujan, Shapiro, Weiss, & Zychlinsky, 2002). The presence of these proteins indicated that the environment surrounding the neutrophils may be inhospitable to *C. jejuni* and limit its growth, which we demonstrated using *in vitro* experiments with purified Lcn2 (with addition of ferric-enterobactin as an iron source), MPO, and Ela2. To further understand how these proteins may be released from neutrophils into gastrointestinal tissues, we first determined the ability of *C. jejuni* to induce neutrophil extracellular traps (NETs) using human and ferret cells.

While many of the above proteins serve as antimicrobials, MPO and Ela2 are also essential for development of NETs (V. Brinkmann, 2004). Using purified human and ferret neutrophils, we observed *C. jejuni* inducing molecular events that precede NETosis, including activation of neutrophils. Upon further investigation of human neutrophils, increased PAD4 expression, histone citrullination, and extrusion of MPO, Ela2, and extracellular DNA was additionally observed. We were able to demonstrate these cellular changes quantitatively and qualitatively, as neutrophils incubated with *C. jejuni* lead to the extrusion of NET-like structures and increases in necessary NET proteins. This provided evidence for NETosis, as these structures do not occur in apoptosis or necrosis. One reason for the decreased expression of PAD4 for PMA induced neutrophils is that these NETs could be produced independent of PAD4 activity. During early research, neutrophils were viewed as terminally differentiated and transcriptionally inert; however, recent research has shown gene regulation and molecular plasticity of neutrophils. In fact, *Helicobacter pylori*, a close relative to *C. jejuni*, causes neutrophil hypersegmentation and subtype differentiation (Whitmore et al., 2017). These results could support the notion of neutrophil plasticity, as *C. jejuni* could cause neutrophils to enter a proinflammatory phenotype. Neutrophil subtype differentiation within the intestinal tissue during campylobacteriosis has yet to be investigated. Further, we demonstrated *C. jejuni* elicits a NET response similar to another well characterized NET inducer, *S. typhimurium*. Curiously, *C. jejuni* and *S. typhimurium*, two bacteria noted for their invasiveness, induced a NET response, while non-invasive *E. coli* O157:H7 did not. As a result, NETs may arise due to bacterial internalization and subsequent intracellular signaling.

Previous research demonstrated that dendritic cell TLR4 recognizes *C. jejuni* LOS and elicits a potent proinflammatory immune response (Kuijf et al., 2010). In addition, TLR4 has been shown to be required for phagocytosis of bacteria by neutrophils (Prokhorenko et al., 2012). Based on these observations, we initially demonstrated that blocking TLR4 on primary human neutrophils decreased *C. jejuni* internalization, which was accompanied by a

reduction in the number of neutrophils undergoing NETosis. Since NETosis was also previously shown to be dependent on TLR4 stimulation independent of internalization, we examined whether *C. jejuni* invasion occurred in neutrophils and impacted NET production. *C. jejuni* invasion into epithelial cells has been studied extensively and found to require the delivery of bacterial effectors like CiaC into the host cell cytosol using the flagellar secretion apparatus (Neal-McKinney & Konkel, 2012). During this process, actin polymerization produces actin-rich cell surface projections which envelop and internalize the bacterium (Carabeo, 2011). The Δ*flgE* mutant of *C. jejuni* does not encode a flagellar hook and is non-flagellated as a result, which leads to defective effector secretion and epithelial cell invasion (Neal-McKinney & Konkel, 2012). Using this strain, we found that internalization into neutrophils was significantly reduced and that the number of NET releasing cells decreased. While *C. jejuni* LOS synthesis is not influenced by deletion of *flgE*, these systems share modification enzymes, including a phosphoethanolamine (pEtN) transferase, which has been shown to protect against cationic antimicrobial peptides and assist in innate immune evasion (Cullen & Trent, 2010). Future studies will investigate the role of LOS modifications in strains with flagellar defects since these strains may be able to synthesize LOS. This reduction supports the conclusion that bacterial internalization - potentially independent of proinflammatory signaling - drives NET production during *C. jejuni* infection. Additionally, *C. jejuni* possesses numerous DNases, encoded by the *cdt* and *dns* genes, that are secreted into the environment (Gaasbeek et al., 2009; He et al., 2019). These factors are notably absent in *Salmonella*, which appears to only possess intracellular DNases, and could be the basis for the bactericidal nature of NETs to *Salmonella* (V. Brinkmann, 2004). Further studies will be required to more thoroughly investigate links between neutrophil phagocytosis, *C. jejuni* invasion into neutrophils, and the implications these have on NET production.

Due to the lack of a small animal model that exhibits clinical signs and responses like that of humans, knowledge is limited regarding the host response to *C. jejuni* infection. In addition to previous studies demonstrating that ferrets develop disease similar to humans, we have shown that ferret neutrophils exhibit markers of NETosis when incubated with *C. jejuni*. Limited ferret specific antibodies are available to evaluate all the cellular changes that occur during NETosis; however, immunofluorescence staining of ferret colonic tissues demonstrated Ela2 positive staining that colocalized with DNA. This staining pattern differed from that of other Ela2 positive cells in uninfected tissues, suggesting that NET responses do occur within colonic tissue during infection. These observations are supported by previous work, which demonstrated neutrophils induce intestinal crypt abscesses in a hyperinflammatory IL-$10^{-/-}$ mouse model of campylobacteriosis (Sun et al., 2013). Using purified human neutrophils and NET inducing conditions, we demonstrated that the combination of *C. jejuni* and neutrophils leads to increased colonocyte cytotoxicity. This cytotoxicity could explain the hallmark histopathology seen within intestinal tissue during campylobacteriosis. As a result, further work is being conducted to determine whether damage to the epithelial cells during *C. jejuni* infection could be due to neutrophil transmigration and subsequent NET induction.

In summary, diarrheal diseases resulting from enteric pathogens are a leading cause of morbidity and mortality in the world, with Campylobacter as the leading cause for

bacterially induced gastroenteritis (Blutt & Estes, 2019). While several of these pathogens have been identified as potent inducers of NETs, there is a gap in knowledge as to the role of NETs in infectious gastroenteritis. This study highlights the importance of neutrophils in the host response to *C. jejuni* infection and how unique activities during infection may drive neutrophil responses that ultimately harm host tissues. Numerous studies have demonstrated that neutrophil accumulation in various inflammatory diseases is accompanied by increased pathology (Fournier & Parkos, 2012). In addition, the induction of NET formation has been correlated with poorer disease outcomes, including several postinfectious disorders associated with *C. jejuni* infection, such as irritable bowel disease (IBD) and rheumatoid arthritis (RA). As a result, further work will be conducted to determine the contribution of *C. jejuni*-induced NET formation on the manifestation of these post-infectious disorders. In addition, leveraging of anti-NET therapeutics may hold potential for resolving acute inflammation during *C. jejuni* infection and/or ameliorating chronic or post-infectious outcomes.

Supplementary Material

Refer to Web version on PubMed Central for supplementary material.

Acknowledgments and author contributions

The authors would like to thank Dr. Caitlin Murphy at the University of Nebraska Medical Center for providing patient fecal samples, Trevor Hancock and Dr. Joseph Jackson for assisting in neutrophil isolation and flow cytometry assistance, Dr. John Dunlap at the UTK Advanced Microscopy and Imaging Center for imaging NETs, Dr. Sarah Lebeis for help with ferret histopathology scoring, and Dr. David Hendrixson at UT Southwestern for supplying the *C. jejuni* 81–176 *flgE* mutant. Immunofluorescence microscopy to evaluate for tissue NETs were performed in part through use of the Vanderbilt Cell Imaging Shared Resource (supported by NIH grants CA68485, DK20593, DK58404, DK59637 and EY08126). This work has been funded by the National Institutes of Health grant R01 HD090061 (to J.A.G.), Career Development Award IK2BX001701 (to J.A.G) from the Office of Medical Research, Department of Veterans Affairs. Additional support for J.A.G. was provided by NIH U01TR002398, NIH R01AI134036 and the Vanderbilt University Medical Center's Digestive Disease Research Center, supported by NIH grant P30DK058404 (Scholarship and Pilot Grant to J.A.G.) and from Vanderbilt Institute for Clinical and Translational Research program supported by the National Center for Research Resources, Grant UL1 RR024975–01, and the National Center for Advancing Translational Sciences, Grant 2 UL1 TR000445–06. R.S.D. was supported by a Vanderbilt University Medical Center Faculty Research Scholars Award and K08Al151100.

References

Akhtar R, Chaudhary Z, & He Y (2010). Modified Method for Isolation of Peripheral Blood Neutrophils from Bovines and Humans. International Journal for Agro Veterinary and Medical Sciences, 4(1), 8 10.5455/ijavms.20101202023635

Bachman MA, Miller VL, & Weiser JN (2009). Mucosal Lipocalin 2 Has Pro-Inflammatory and Iron-Sequestering Effects in Response to Bacterial Enterobactin. PLoS Pathogens, 5(10), e1000622 10.1371/journal.ppat.1000622 [PubMed: 19834550]

Backert S, Boehm M, Wessler S, & Tegtmeyer N (2013). Transmigration route of Campylobacter jejuni across polarized intestinal epithelial cells: Paracellular, transcellular or both? Cell Communication and Signaling, 11(1), 72 10.1186/1478-811X-11-72 [PubMed: 24079544]

Black RE, Levine MM, Clements ML, Hughes TP, & Blaser MJ (1988). Experimental Campylobacter jejuni Infection in Humans. Journal of Infectious Diseases, 157(3), 472–479. 10.1093/infdis/157.3.472 [PubMed: 3343522]

Blutt SE, & Estes MK (2019). Gut Bacterial Bouncers: Keeping Viral Pathogens out of the Epithelium. Cell Host & Microbe, 26(5), 569–570. 10.1016/j.chom.2019.10.018 [PubMed: 31726023]

Brinkmann V (2004). Neutrophil Extracellular Traps Kill Bacteria. Science, 303(5663), 1532–1535. 10.1126/science.1092385 [PubMed: 15001782]

Brinkmann Volker, Abu Abed U, Goosmann C, & Zychlinsky A (2016). Immunodetection of NETs in Paraffin-Embedded Tissue. Frontiers in Immunology, 7 10.3389/fimmu.2016.00513

Brinkmann Volker, Laube B, Abu Abed U, Goosmann C, & Zychlinsky A (2010). Neutrophil Extracellular Traps: How to Generate and Visualize Them. Journal of Visualized Experiments, (36), 1724 10.3791/1724 [PubMed: 20182410]

Carabeo R (2011). Bacterial subversion of host actin dynamics at the plasma membrane: Bacterial subversion of host actin dynamics. Cellular Microbiology, 13(10), 1460–1469. 10.1111/j.1462-5822.2011.01651.x [PubMed: 21790944]

Chassaing B, Srinivasan G, Delgado MA, Young AN, Gewirtz AT, & Vijay-Kumar M (2012). Fecal Lipocalin 2, a Sensitive and Broadly Dynamic Non-Invasive Biomarker for Intestinal Inflammation. PLoS ONE, 7(9), e44328 10.1371/journal.pone.0044328 [PubMed: 22957064]

Coburn B, Sekirov I, & Finlay BB (2007). Type III Secretion Systems and Disease. Clinical Microbiology Reviews, 20(4), 535–549. 10.1128/CMR.00013-07 [PubMed: 17934073]

Copenhaver AM, Casson CN, Nguyen HT, Fung TC, Duda MM, Roy CR, & Shin S (2014). Alveolar Macrophages and Neutrophils Are the Primary Reservoirs for Legionella pneumophila and Mediate Cytosolic Surveillance of Type IV Secretion. Infection and Immunity, 82(10), 4325–4336. 10.1128/IAI.01891-14 [PubMed: 25092908]

Crofts AA, Poly FM, Ewing CP, Kuroiwa JM, Rimmer JE, Harro C, … Trent MS (2018). Campylobacter jejuni transcriptional and genetic adaptation during human infection. Nature Microbiology, 3(4), 494–502. 10.1038/s41564-018-0133-7

Cullen TW, & Trent MS (2010). A link between the assembly of flagella and lipooligosaccharide of the Gram-negative bacterium Campylobacter jejuni. Proceedings of the National Academy of Sciences, 107(11), 5160–5165. 10.1073/pnas.0913451107

Dale DC, Boxer L, & Liles WC (2008). The phagocytes: Neutrophils and monocytes. Blood, 112(4), 935–945. 10.1182/blood-2007-12-077917 [PubMed: 18684880]

Doster RS, Sutton JA, Rogers LM, Aronoff DM, & Gaddy JA (2018). Streptococcus agalactiae Induces Placental Macrophages To Release Extracellular Traps Loaded with Tissue Remodeling Enzymes via an Oxidative Burst-Dependent Mechanism. MBio, 9(6), e02084–18. 10.1128/mBio.02084-18 [PubMed: 30459195]

Erpenbeck L, & Schön MP (2017). Neutrophil extracellular traps: Protagonists of cancer progression? Oncogene, 36(18), 2483–2490. 10.1038/onc.2016.406 [PubMed: 27941879]

Fournier BM, & Parkos CA (2012). The role of neutrophils during intestinal inflammation. Mucosal Immunology, 5(4), 354–366. 10.1038/mi.2012.24 [PubMed: 22491176]

Fukuto HS, & Bliska JB (2014). Yersinia pestis survives in neutrophils and sends a PS to macrophages: Bon appétit! Journal of Leukocyte Biology, 95(3), 383–385. 10.1189/jlb.1013556 [PubMed: 24586037]

Gaasbeek EJ, Wagenaar JA, Guilhabert MR, Wosten MMSM, van Putten JPM, van der Graaf-van Bloois L, Parker CT, & van der Wal FJ (2009). A DNase Encoded by Integrated Element CJIE1 Inhibits Natural Transformation of Campylobacter jejuni. Journal of Bacteriology, 191(7), 2296–2306. 10.1128/JB.01430-08 [PubMed: 19151136]

He Y, Yang F-Y, & Sun E-W (2018). Neutrophil Extracellular Traps in Autoimmune Diseases: Chinese Medical Journal, 131(13), 1513–1519. 10.4103/0366-6999.235122 [PubMed: 29941703]

He Z, Gharaibeh RZ, Newsome RC, Pope JL, Dougherty MW, Tomkovich S, Pons B, Mirey G, Vignard J, Hendrixson DR, & Jobin C (2019). Campylobacter jejuni promotes colorectal tumorigenesis through the action of cytolethal distending toxin. Gut, 68(2), 289–300. 10.1136/gutjnl-2018-317200 [PubMed: 30377189]

Klebanoff SJ (2005). Myeloperoxidase: Friend and foe. Journal of Leukocyte Biology, 77(5), 598–625. 10.1189/jlb.1204697 [PubMed: 15689384]

Kolaczkowska E, & Kubes P (2013). Neutrophil recruitment and function in health and inflammation. Nature Reviews Immunology, 13(3), 159–175. 10.1038/nri3399

Kuijf ML, Samsom JN, van Rijs W, Bax M, Huizinga R, Heikema AP, … Jacobs BC (2010). TLR4-Mediated Sensing of Campylobacter jejuni by Dendritic Cells Is Determined by Sialylation. The Journal of Immunology, 185(1), 748–755. 10.4049/jimmunol.0903014 [PubMed: 20525894]

Lebeis SL, Powell KR, Merlin D, Sherman MA, & Kalman D (2009). Interleukin-1 Receptor Signaling Protects Mice from Lethal Intestinal Damage Caused by the Attaching and Effacing Pathogen Citrobacter rodentium. Infection and Immunity, 77(2), 604–614. 10.1128/IAI.00907-08 [PubMed: 19075023]

Man SM (2011). The clinical importance of emerging Campylobacter species. Nature Reviews Gastroenterology & Hepatology, 8(12), 669–685. 10.1038/nrgastro.2011.191 [PubMed: 22025030]

Neal-McKinney JM, & Konkel ME (2012). The Campylobacter jejuni CiaC virulence protein is secreted from the flagellum and delivered to the cytosol of host cells. Frontiers in Cellular and Infection Microbiology, 2 10.3389/fcimb.2012.00031

Negretti NM, & Konkel ME (2017). Methods to Study Campylobacter jejuni Adherence to and Invasion of Host Epithelial Cells In Butcher J & Stintzi A (Eds.), Campylobacter jejuni (Vol. 1512, pp. 117–127). 10.1007/978-1-4939-6536-6_11

Nemelka KW, Brown AW, Wallace SM, Jones E, Asher LV, Pattarini D, … Baqar S (2009). Immune response to and histopathology of Campylobacter jejuni infection in ferrets (Mustela putorius furo). Comparative Medicine, 59(4), 363–371. [PubMed: 19712577]

Papayannopoulos V (2018). Neutrophil extracellular traps in immunity and disease. Nature Reviews Immunology, 18(2), 134–147. 10.1038/nri.2017.105

Prokhorenko I, Zubova S, Kabanov D, Voloshina E, & Grachev S (2012). Toll-like receptor 4 in phagocytosis of Escherichia coli by endotoxin-activated human neutrophils in whole blood. Critical Care, 16(Suppl 3), P80 10.1186/cc11767

Rathinam VAK, Appledorn DM, Hoag KA, Amalfitano A, & Mansfield LS (2009). Campylobacter jejuni-Induced Activation of Dendritic Cells Involves Cooperative Signaling through Toll-Like Receptor 4 (TLR4)-MyD88 and TLR4-TRIF Axes. Infection and Immunity, 77(6), 2499–2507. 10.1128/IAI.01562-08 [PubMed: 19332531]

Reti KL, Tymensen LD, Davis SP, Amrein MW, & Buret AG (2015). Campylobacter jejuni Increases Flagellar Expression and Adhesion of Noninvasive Escherichia coli: Effects on Enterocytic Toll-Like Receptor 4 and CXCL-8 Expression. Infection and Immunity, 83(12), 4571–4581. 10.1128/IAI.00970-15 [PubMed: 26371123]

Saffarzadeh M, Juenemann C, Queisser MA, Lochnit G, Barreto G, Galuska SP, … Preissner KT (2012). Neutrophil Extracellular Traps Directly Induce Epithelial and Endothelial Cell Death: A Predominant Role of Histones. PLoS ONE, 7(2), e32366 10.1371/journal.pone.0032366 [PubMed: 22389696]

Shank JM, Kelley BR, Jackson JW, Tweedie JL, Franklin D, Damo SM, … Johnson JG (2018). The Host Antimicrobial Protein Calgranulin C Participates in the Control of Campylobacter jejuni Growth via Zinc Sequestration. Infection and Immunity, 86(6), e00234–18, /iai/86/6/e00234-18.atom. 10.1128/IAI.00234-18 [PubMed: 29610259]

Silva J, Leite D, Fernandes M, Mena C, Gibbs PA, & Teixeira P (2011). Campylobacter spp. as a Foodborne Pathogen: A Review. Frontiers in Microbiology, 2 10.3389/fmicb.2011.00200

Stahl M, & Vallance BA (2015). Insights into Campylobacter jejuni colonization of the mammalian intestinal tract using a novel mouse model of infection. Gut Microbes, 6(2), 143–148. 10.1080/19490976.2015.1016691 [PubMed: 25831043]

Storisteanu DML, Pocock JM, Cowburn AS, Juss JK, Nadesalingam A, Nizet V, & Chilvers ER (2017). Evasion of Neutrophil Extracellular Traps by Respiratory Pathogens. American Journal of Respiratory Cell and Molecular Biology, 56(4), 423–431. 10.1165/rcmb.2016-0193PS [PubMed: 27854516]

Sun X, Liu B, Sartor RB, & Jobin C (2013). Phosphatidylinositol 3-Kinase-γ Signaling Promotes Campylobacter jejuni –Induced Colitis through Neutrophil Recruitment in Mice. The Journal of Immunology, 190(1), 357–365. 10.4049/jimmunol.1201825 [PubMed: 23180818]

Tan Y, Zanoni I, Cullen TW, Goodman AL, & Kagan JC (2015). Mechanisms of Toll-like Receptor 4 Endocytosis Reveal a Common Immune-Evasion Strategy Used by Pathogenic and Commensal Bacteria. Immunity, 43(5), 909–922. 10.1016/j.immuni.2015.10.008 [PubMed: 26546281]

Watson RO, & Galán JE (2008). Campylobacter jejuni Survives within Epithelial Cells by Avoiding Delivery to Lysosomes. PLoS Pathogens, 4(1), e14 10.1371/journal.ppat.0040014 [PubMed: 18225954]

Weinrauch Y, Drujan D, Shapiro SD, Weiss J, & Zychlinsky A (2002). Neutrophil elastase targets virulence factors of enterobacteria. Nature, 417(6884), 91–94. 10.1038/417091a [PubMed: 12018205]

Whitmore LC, Weems MN, & Allen LH (2017). Cutting Edge: Helicobacter pylori Induces Nuclear Hypersegmentation and Subtype Differentiation of Human Neutrophils In Vitro. Journal of immunology (Baltimore, Md. : 1950), 198(5), 1793–1797. 10.4049/jimmunol.1601292

World Health Organization (Ed.). (2015). WHO estimates of the global burden of foodborne diseases. Geneva, Switzerland: World Health Organization.

Young KT, Davis LM, & DiRita VJ (2007). Campylobacter jejuni: Molecular biology and pathogenesis. Nature Reviews Microbiology, 5(9), 665–679. 10.1038/nrmicro1718 [PubMed: 17703225]

Zharkova O, Tay SH, Lee HY, Shubhita T, Ong WY, Lateef A, … Fairhurst A (2019). A Flow Cytometry-Based Assay for High-Throughput Detection and Quantification of Neutrophil Extracellular Traps in Mixed Cell Populations. Cytometry Part A, 95(3), 268–278. 10.1002/cyto.a.23672

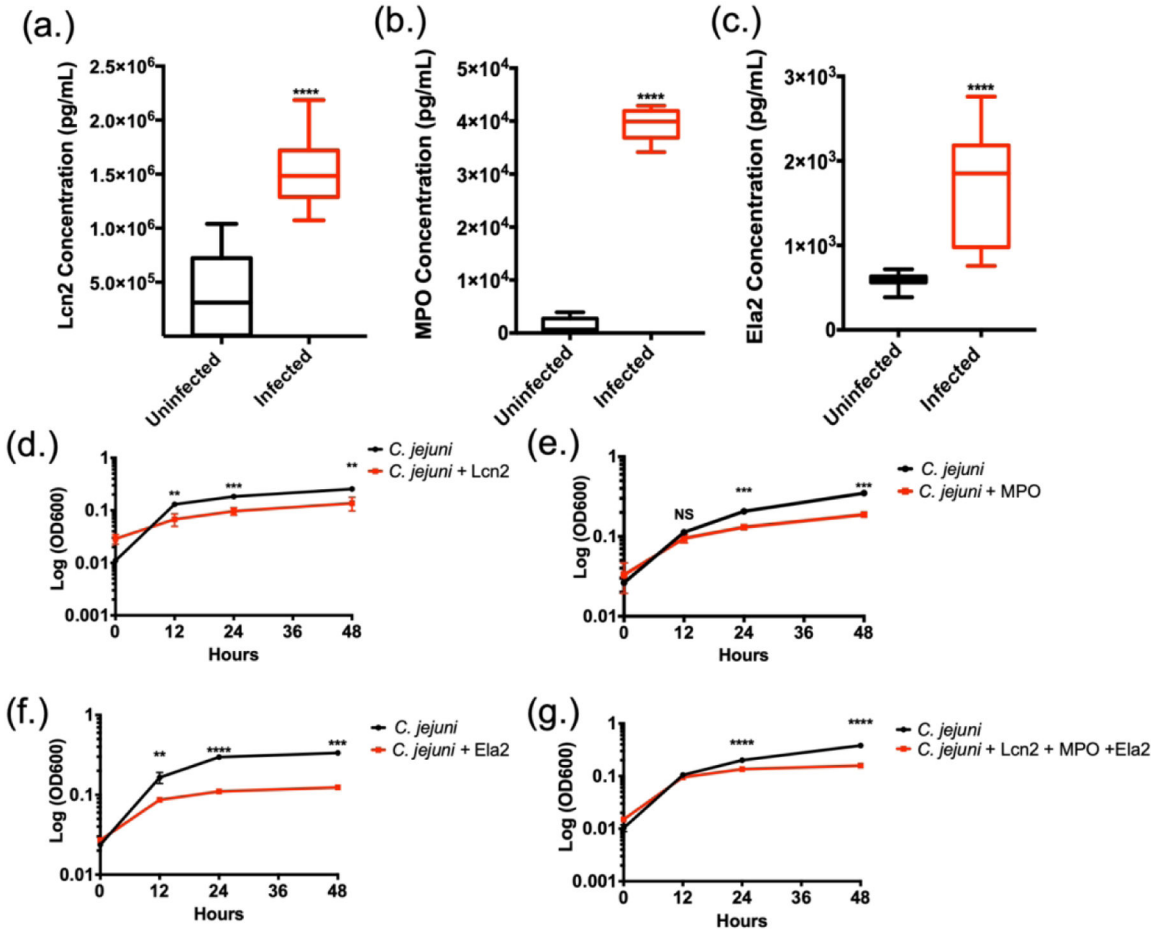

Figure 1.

Neutrophil-derived antimicrobial proteins and NET components accumulate in *C. jejuni*-infected patient fecal samples. (A-C) Lipocalin-2 (Lcn2), myeloperoxidase (MPO), and neutrophil elastase (Ela2) protein levels significantly increases in infected individuals. (D-F) Neutrophil-derived proteins decrease *C. jejuni* growth for up to 48 hours. (G) Granule proteins synergistically decrease *C. jejuni* growth *in vitro*. Statistical analyses of representative fecal samples were performed using a nonparametric Mann-Whitney U test between uninfected and infected groups. Statistical analysis of growth curves performed using an unpaired t test between *C. jejuni* and *C. jejuni* - antimicrobial groups. ** $p < 0.01$; *** $p < 0.001$; **** $p < 0.0001$.

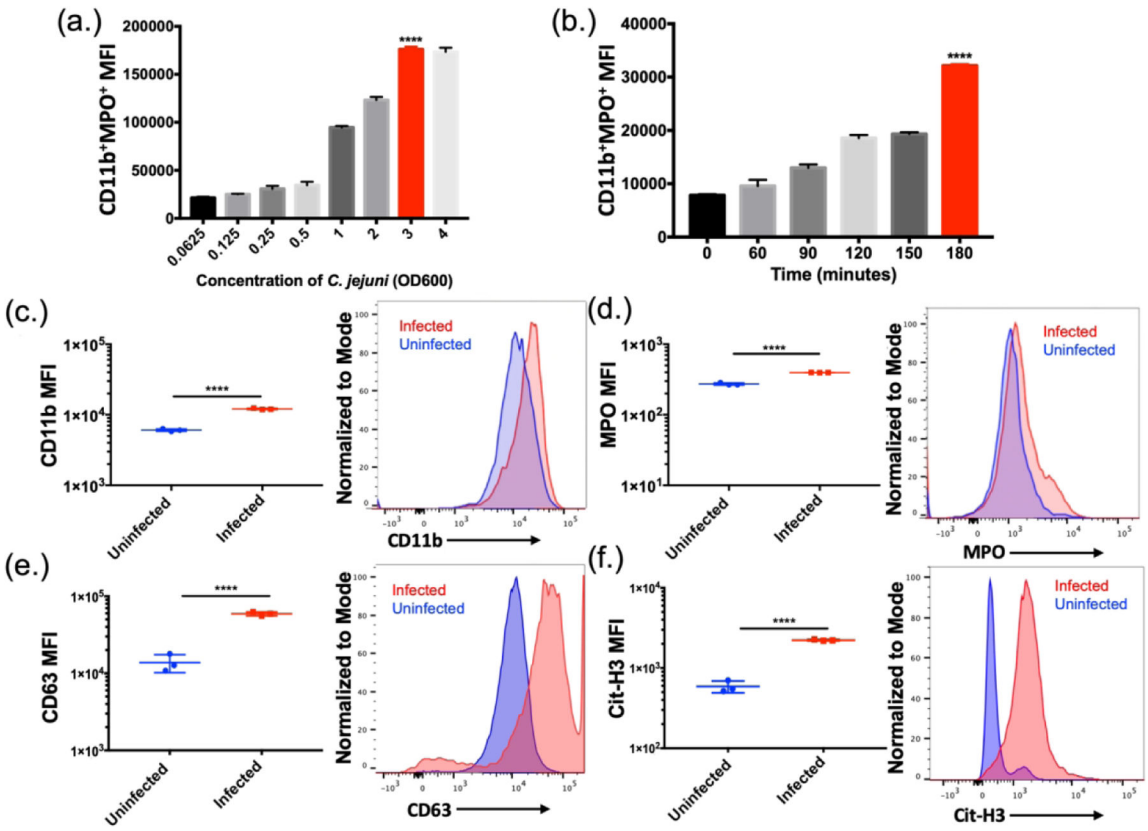

Figure 2.

Flow cytometry analysis of *C. jejuni* induced NETs (A) Neutrophils exhibited increased NET production up until an OD600 of 3.0 (B) Neutrophils exhibited increased NET production when incubated with *C. jejuni* up to three hours. Flow cytometry analysis of human neutrophil activation using CD11b (C), extracellular expression of MPO (D), CD63 (E), and citrullinated histone 3 (Cit-H3) (F). Expression of each marker was normalized to the mode of the population. Results are expressed as representative data of biological and technical triplicates. Statistical analysis was performed using an unpaired t test between uninfected and infected groups. $^{**}p < 0.01$; $^{***}p < 0.001$; $^{****}p < 0.0001$.

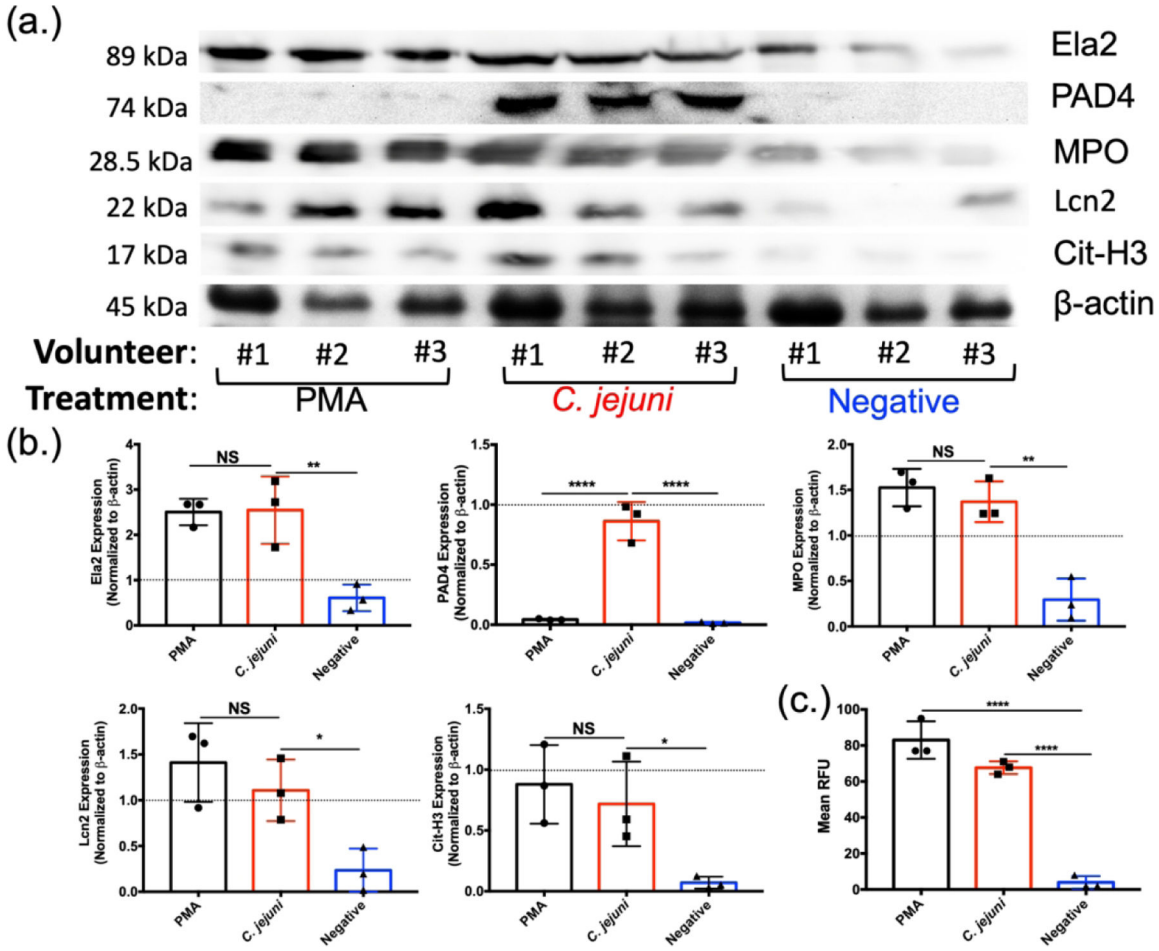

Figure 3:

Western blot analysis of essential NET components. Volunteer neutrophils were incubated with PMA (positive control), wild-type *C. jejuni*, or media (negative control). (A) Western blot detection of neutrophil elastase (Ela2), PAD4, myeloperoxidase (MPO), lipocalin-2 (Lcn2), citrullinated histone H3 (Cit-H3), and β-actin as a loading control. (B) Densitometry quantification of NET components relative to beta actin density. (C) SYTOX assay to detect extracellular DNA. Results are expressed as representative data of biological and technical triplicates. Statistical analysis was performed using an unpaired t test between PMA, *C. jejuni*, and negative treated neutrophils. Multiple comparison testing was performed using ANOVA with post hoc test. $*p < 0.05$; $**p < 0.01$; $***p < 0.001$; $****p < 0.0001$.

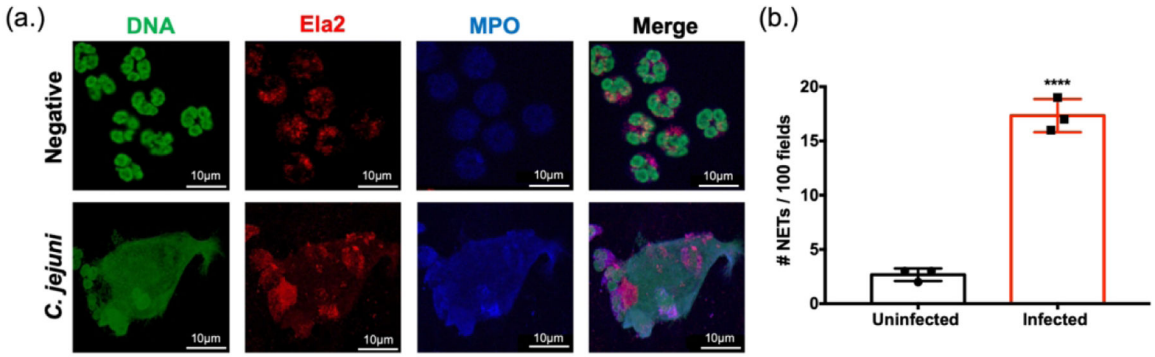

Figure 4:

Visualization of *C. jejuni*-induced NETs using fluorescent microscopy. (A) Images were individually taken at the appropriate wavelength for each fluorescent antibody following incubation with wild-type *C. jejuni* or media alone (negative). Representative images for each marker were then merged to visualize NET components, including extracellular DNA. (B) NET production was assessed for 100 fields from three separate neutrophil purifications. Scale bars are 10 μm. Results are expressed as representative data of biological and technical triplicates. Statistical analysis was performed using an unpaired t test between uninfected and infected groups. ****$p < 0.0001$.

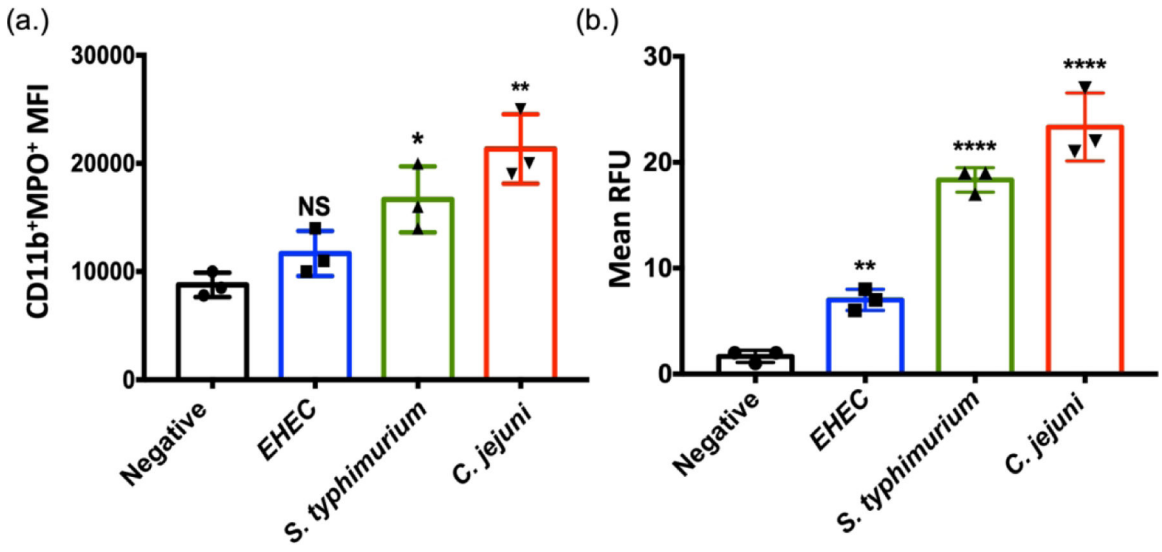

Figure 5:

Comparison of NET production by other gastrointestinal pathogens. (A) Flow cytometry analysis of Cd11b and myeloperoxidase (MPO) markers accumulating on human neutrophils following incubation with either media alone (negative), *E. coli* O157:H7, *S. typhimurium* SL1344, or wild-type *C. jejuni*. (B) SYTOX assay detecting extracellular DNA from neutrophils incubated from three separate volunteers. Results are expressed as representative data of biological and technical triplicates. Statistical analysis was performed using an unpaired t test between negative, *EHEC*, *S. typhimurium*, and *C. jejuni* stimulated neutrophil groups. Multiple comparison testing was performed using ANOVA with post hoc test. $*p < 0.05$; $**p < 0.01$; $****p < 0.0001$.

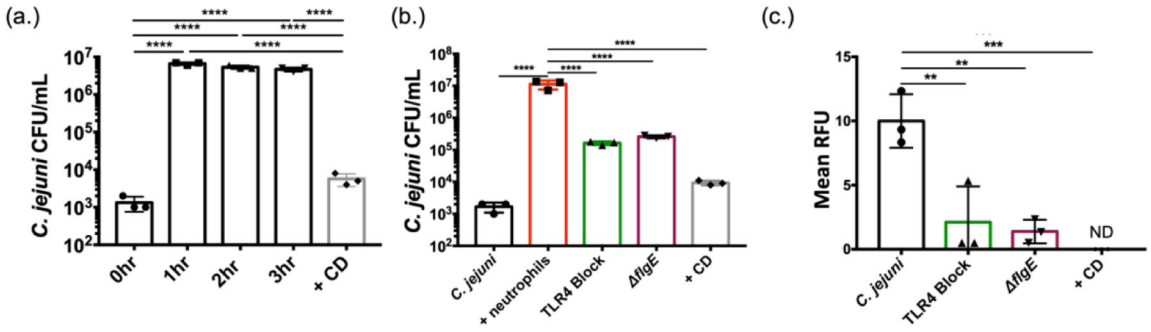

Figure 6:

Neutrophil phagocytosis and internalization of *C. jejuni*. (A) Gentamicin protection assay of *C. jejuni* within neutrophils for varying amounts of time and cytochalasin D (CD). (B) Gentamicin protection assay of neutrophils lacking functional TLR4 and neutrophils incubated with flagellar mutants. (C) SYTOX assay to detect extracellular nucleic acids of neutrophils lacking functional TLR4 and neutrophils incubated with flagellar mutants. Results are expressed as representative data of biological and technical triplicates. Statistical analysis was performed using an unpaired t test between *C. jejuni* stimulated neutrophil groups. Multiple comparison testing was performed using ANOVA with post hoc test. $*p < 0.05$; $**p < 0.01$; $***p < 0.001$; $****p < 0.0001$.

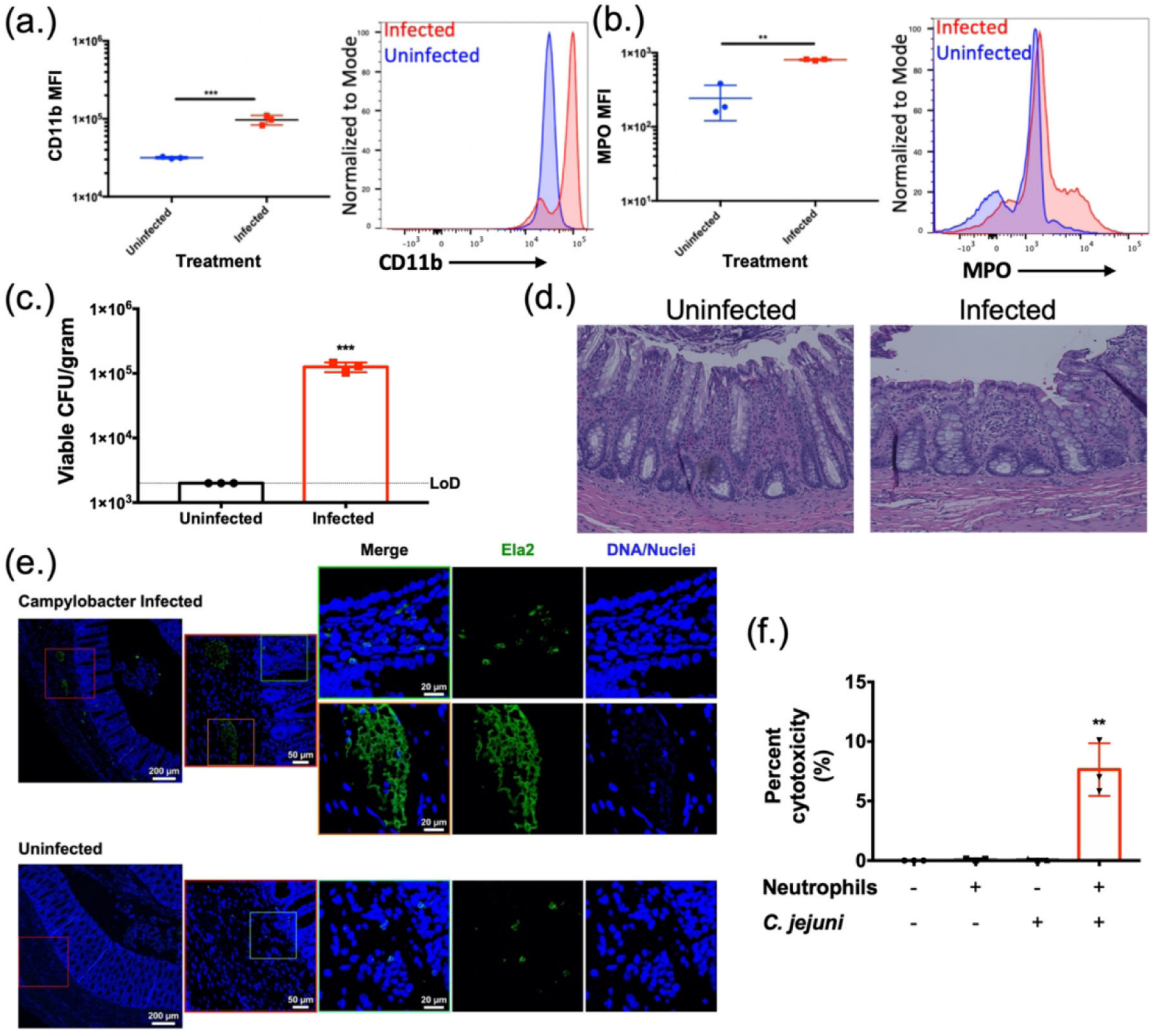

Figure 7:

Histopathology of ferret tissues and cytotoxicity of *C. jejuni* induced NETs. Flow cytometry analysis of ferret neutrophil activation using CD11b (A) and extracellular expression of MPO (B). (C) Fecal loads of *C. jejuni* infected ferrets day three post infection. (D) H&E stained *C. jejuni* infected ferret colon exhibiting signs of pathology. (E) Immunofluorescent analysis of ferret colon tissue for NETs. Ferret colon tissues were stained using anti- Ela2 antibodies (green) or Hoechst for DNA (blue) and were examined by confocal microscopy. In *C. jejuni* infected colonic tissues several collections of Ela2 staining projections were noted just below the colonic crypts but were not seen in uninfected tissues (red boxes) Higher magnification of these collections (orange box) demonstrated extended Ela2 projections that colocalized with DNA staining, suggestive of NET structures. In the villi of infected animals and in the mucosa of uninfected animals, Ela2 positive cells were noted with intact nuclei and punctate Ela2 staining (green boxes). (F) LDH assay of colonic HCT116 cells incubated with *C. jejuni* induced NETs. Results are expressed as representative data of biological and technical triplicates. Statistical analysis was performed

using an unpaired t test between uninfected and infected groups. *$p < 0.05$; **$p < 0.01$; ***$p < 0.001$.